Progressive Nuclear Translocation of Somatostatin Analogs

Conrad A. Hornick, Catherine T. Anthony, Susan Hughey, Bryan M. Gebhardt, Gregory D. Espenan, and Eugene A. Woltering

Departments of Physiology, Pathology, Surgery, Ophthalmology, and Radiology, The Stanley S. Scott Cancer Center; Neuroscience Center of Excellence, Louisiana State University Medical Center, New Orleans; and Veterans Administration Medical Center, New Orleans, Louisiana

Optimal cancer radiotherapy using Auger electron emitters requires selective localization of radionuclides in close proximity to tumor DNA. **Methods:** Intracellular trafficking of ^{125}I-Tyr^{1}-somatostatin-14 somatotropin-release inhibiting factor (SRIF) and 2 of its analogs, ^{125}I-WOC 4a and ^{111}In-pentetreotide, was studied in human neuroblastoma cells. **Results:** After 24-h incubation, SRIF was degraded or recycled, whereas its protease-resistant analogs progressively accumulated in nuclear fractions. ^{111}In-pentetreotide binding to DNA increased over time in somatostatin receptor–positive cells but not in somatostatin receptor–negative cells. **Conclusion:** These in vitro studies show that prolonged exposure to radiolabeled SRIF analogs significantly increases their cellular internalization, nuclear translocation, and DNA binding. Clinically, infusion of radiolabeled somatostatin analogs may enhance tumor uptake and retention and provide more effective in situ radiotherapy.

Key Words: somatostatin; membrane receptor; DNA binding; endocytosis; in situ radiotherapy

J Nucl Med 2000; 41:1256–1263

The tetradecapeptide somatostatin initiates both antisecretory and antiproliferative effects in a variety of tissue types. Somatostatin binding to cells is mediated by 5 distinct somatostatin receptor proteins (sst-1–5) (*1*). These receptors are highly homologous and have in common a G-protein mode of signal transduction (*2*). Earlier work, by Lamberts et al. (*3*), showed a higher concentration of somatostatin receptors on endocrine tumor cells than on normal cells. Several nonendocrine malignancies have also been shown to overexpress these receptors (*4*). Recently, protease-resistant radiolabeled somatostatin analogs have been used as treatment for somatostatin-expressing tumors (*5–8*). To optimize the clinical potential of these ligands for in situ radiation therapy, one must follow their intracellular movements. This is important to determine their mechanisms of action and to determine if modification of their intracellular destination can prolong cellular retention time and optimize in situ radiotherapy. For Auger electron emitters such as ^{125}I or ^{111}In, which produce low-energy, short-range radiation effects (<10 mm), to be effective antitumor agents, localization within the nuclei in close proximity to cellular DNA is necessary to obtain maximum cytotoxicity (*9,10*).

Earlier research has shown that the somatostatin receptor complex can be internalized by receptor-mediated endocytosis (*11*). Many peptide receptors, with or without attached ligands, can return from endosomes to the plasma membrane through a budding process that forms recycling vesicles or retrosomes concomitant with acidification of the endosome interior and a change in membrane lipid composition (*12*). Although pathways from the endosomal compartment back to the plasmalemma through retrosomes or on to lysosomal degradation are found in many cell types, other intracellular destinations for ligands entering cells by receptor-mediated endocytosis have also been described. Traffic between endosomes and the Golgi complex is well documented (*13*), and transcytosis, or the movement of ligands in endocytic vesicles from the plasmalemma to another cell surface, has also been shown (*14*). However, a pathway linking endosomes and the nucleus has never been elucidated.

Substantial evidence exists that both ligand composition and receptor subtype are critical factors in the intracellular routing and retention of somatostatin and its analogs. Roth et al. (*15*) observed that of the 5 cloned somatostatin receptors transfected into human embryonic kidney cells, only sst-1 through sst-3 were capable of promoting endocytosis of the somatostatin receptor complex after binding of either native sst-14 or sst-28. The sst-5 receptor entered cells only after binding the octacosapeptide, whereas sst-4 remained at the cell surface in the presence of both ligands. Studies by Nouel et al. (*16*) using fluorescence confocal microscopy and the stable somatostatin analog, (D-Trp^{8})-somatotropin-release inhibiting factor (SRIF), have determined that the intracellular pathways followed by somatostatin receptor complexes that have been taken up into cells transfected with sst-1 and sst-2 were clearly distinct. In sst-1 transfected cells, the receptor–ligand complex remained near the plasma membrane after internalization. In sst-2 transfected cells, the complex moved down the endocytic pathway to the nuclear region. In contrast, using the stable cyclic hexapeptide

Received Jul. 9, 1999; revision accepted Oct. 27, 1999.

For correspondence or reprints contact: Eugene A. Woltering, MD, Medical Center at New Orleans, 1542 Tulane Ave., T7-1, New Orleans, LA 70112.

somatostatin agonist ^{125}I-BIM-23027, the sst-2 receptor–ligand complex in Neuro2A cells has been shown to rapidly recycle to the cell surface within 20 min after internalization (*17*). The result is a relatively low intracellular concentration of radioligand maintained as a balance between endo- and exocytosis. Using stable CHO-K1 cells, Hukovic et al. (*18*) found that radioligand internalization was most effective with sst-3 and less effective with sst-5, -4 and -2, whereas sst-1 showed no cellular internalization. Taken together, these studies indicate that signal transduction pathways regulating internalization may vary with both cell line and receptor subtype. Thus, somatostatin receptors transfected into various types of cells may not mimic the in vivo activity of the native receptor.

In the studies presented here, we show that prolonged exposure of the human neuroblastoma IMR-32 cell line expressing native sst-2 to radiolabeled somatostatin analogs leads to progressive accumulation of radioligand in the nuclear compartment. Moreover, the gradual translocation of radioligand from other intracellular sites to the nucleus is paralleled by a dramatic rise in binding to DNA in somatostatin-positive but not somatostatin-negative cells. These findings support the intracellular movement of peptides from the endocytic compartment into the nucleus. These findings also imply that prolonged infusional therapy with stable radiolabeled somatostatin analogs should promote intracellular accumulation, increase cellular retention of radioligand, and optimize energy transfer from Auger electron emitters to tumor DNA.

MATERIALS AND METHODS

Cell Culture

IMR-32 cells (American Type Tissue Company, Bethesda, MD) and SKNSH cells (M. Sue O'Dorisio, Ohio State University, Columbus, OH) were maintained in growth medium consisting of minimal essential medium with glutamine, supplemented with nonessential amino acids, fetal bovine serum, antibiotics, and antimycotics (GIBCO, Grand Island, NY). Growth medium was replaced every 2–3 d. Cells were maintained at 37°C in a humidified environment with 5% CO_2. Both IMR-32 and SKNSH are human neuroblastoma cells. IMR-32 possesses the sst-2 receptor, whereas SKNSH lacks somatostatin receptors (*19*).

Whole-Cell Binding Assay

Harvested cells were counted and added to sterile borosilicate glass assay tubes (12 × 75 mm) at a concentration of 500,000 cells per tube. Cells were prepared 1 d before initiation of the assay. To initiate the assay, the growth medium was replaced with binding buffer (minimal essential medium supplemented with 10 mmol/L *N*-2-hydroxyethylpiperazine-*N*-2-ethanesulfonic acid and 0.1% bovine serum albumin) containing radioligand (500,000 cpm) in 1 mL (7 pmol/L ^{111}In-pentetreotide:66 pmol/L ^{125}I-WOC 4a). Parallel incubations containing radioligand with an excess of nonradioactive octreotide acetate (1 μmol/L) were included to determine nonspecific binding. Incubations were prepared in triplicate without (total) or with (nonspecific) 1 μmol/L octreotide acetate and incubated for specified times at 37°C in a 5% CO_2 and 95% air environment. With the exception of time required for determination of radioactivity in the γ counter, the cells were maintained at 4°C throughout the rest of the experiment. To terminate the incubations, the tubes were placed on ice, the incubation buffer was aspirated, and the cells were rinsed twice with ice-cold Hank's balanced salt solution (HBSS; pH 7.6). The cells were transferred to a new tube, and the bound radioactivity was determined using a γ counter (model 5500; Beckman, Palo Alto, CA). The level of radioactivity (cpm) averaged from triplicate tubes represented total cell binding. The cells were centrifuged, the supernate was aspirated, and the cells were incubated with HBSS, pH 4.0, for 10 min at 4°C. After a rinse with HBSS, the level of radioactivity was again determined using a γ counter. This level represented intracellular binding. Membrane binding was calculated as the difference between total binding and intracellular binding. Specific binding (total, intracellular, and membrane) was calculated as the difference between radioactive levels without versus with the 1 μmol/L unlabeled octreotide acetate. All binding was corrected for the protein content of the cells to negate the effect of cell proliferation over time.

Cell Culture for Drug Distribution Study

The cells used in experiments that investigated intracellular drug distribution were grown in medium. Flasks containing IMR-32 or SKNSH were incubated with radioligand (154 pmol/L ^{125}I-SRIF-14:7 pmol/L ^{111}In-pentetreotide:66 pmol/L ^{125}I-WOC 4a) for predetermined times and then harvested mechanically or with a 10-min exposure to trypsin-ethylenediaminetetraacetic acid (EDTA) (GIBCO) at 4°C. The cells were formed into pellets, washed twice in serum-containing growth medium, and used in the assays.

Organelle Isolation

For isolation of various cellular organelles, the cells were washed twice in ice-cold phosphate-buffered saline (PBS), resuspended in 4.5 mL 0.25 mol/L sucrose at 4°C, and passed 3 times through a stainless steel ball bearing homogenizer to rupture cell membranes. Isotonic Percoll (Sigma Chemical Co., St. Louis, MO), at pH 7.2, containing density marker beads (Pharmacia, Uppsala, Sweden) was added to the mixture to achieve a concentration of 0.292 (volume per volume). Centrifugation at 20,400 rpm and 4°C, in a fixed-angle 40.2 rotor (Beckman), resulted in a gradient that was clearly defined by the marker beads. The gradient was then fractionated (Isco, Inc., Lincoln, NE) into aliquots of approximately 250 μL. Gradient fractions were counted for radioactivity in a γ counter.

Assays

The DNA content in each aliquot was assayed spectrophotometrically at 260 nm using a 100-10 spectrophotometer (Hitachi Medical Corporation of America, Twinsburg, OH) (*20*), and protein was assayed with a Micro BCA protein assay kit (Pierce Chemical Co., Rockford, IL). The 5′ nucleotidase assay used as an enzyme marker for plasma membrane was performed according to the method of Emmelot et al. (*21*). The *N*-acetyl-β-glucosaminidase assay used as an enzyme marker for lysosomes was performed according to the method of Findlay et al. (*22*)

Radiolabeling

^{111}In-pentetreotide (Mallinckrodt Medical, St. Louis, MO) was labeled according to the manufacturer's instructions. ^{125}I-Tyr^{1}-SRIF-14 (New England Nuclear, Boston, MA) and ^{125}I-WOC 4a (David Coy, Tulane University, New Orleans, LA) were labeled, purified, and tested according to published methods (*23*). The specific activities of these peptides were 1721 MBq/mmol for

TABLE 1
Specific Binding and Internalization of ^{111}In-Pentetreotide by IMR-32 Cells Over Time

Parameter	1 h	24 h	48 h	72 h
Total specific binding	4,109 ± 686	45,569 ± 2,105	50,105 ± 2,276	43,498 ± 4,373
Specific intracellular uptake	3,012 ± 371	25,340 ± 365	26,719 ± 2,136	26,917 ± 4,040
Membrane-specific binding	1,101 ± 26	20,229 ± 178	23,386 ± 1,965	16,581 ± 2,972

Specific binding represents difference in counts per minute in triplicate tubes incubated with or without thousandfold excess of octreotide for times shown. Membrane counts were assessed by acid stripping cells (pH 4 × 10 min) after removal of nonspecifically bound label by 2 buffer washes.

^{111}In-pentetreotide, 315 MBq/mmol for ^{125}I-WOC 4a, and 81 MBq/mmol for ^{125}I-Tyr^1-SRIF-14 (*23*).

DNA Binding

IMR-32 (somatostatin-positive) or SKNSH (somatostatin-negative) cells were incubated for various periods with ^{125}I- or ^{111}In-labeled peptide either alone or with the radioligand and an excess of cold competitor. Triplicate T-75 flasks containing cells were mechanically harvested and washed 3 times in Dulbecco's PBS. DNA was extracted from both the cell lines using a genomic preparation tissue DNA isolation kit (Pharmacia Biotech, Piscataway, NJ). DNA from each flask was treated with proteinase (Life Technologies, Gaithersburg, MD) for 1 h at 37° C. DNA was then precipitated again with 100% ethanol and 3 mol/L sodium acetate, washed in cold ethanol, and redissolved in 10 mmol/L Tris-EDTA, pH 7.4. DNA (100 μg) was transferred to counting vials, and the radioactivity associated with each tube was measured in a 5500 γ counter.

RESULTS

Table 1 illustrates the progressive specific binding and internalization of ^{111}In-pentetreotide in IMR-32 human neuroblastoma cells over time. In a typical binding time course, approximately 10% of the administered activity is in the total specifically bound fraction. In Figure 1, the gradient density distributions of both DNA and protein from homogenized IMR-32 cells are plotted. These data show that the cell nuclei are localized in the more dense regions of the gradient. Protein peaks are widely distributed but occur chiefly in both the lighter and the heavier portions of the gradient. Figure 2 plots the gradient distributions of 5′ nucleotidase (*21*) and *N*-acetyl-β-glucosaminidase (*22*), enzyme markers for the plasma membrane and lysosomes, respectively. The enzyme distributions show that plasma membrane is concentrated in the less dense fractions of the gradient, whereas lysosomes are chiefly found in fractions 13 through 15 at higher gradient densities. Figures 3, 4, and 5 contrast the intracellular distribution over time of ^{125}I-labeled Tyr^1-sst-14, ^{125}I-labeled WOC 4a, and ^{111}In-pentetreotide, respectively. The distribution of labeled sst-14 shows a small initial buildup in both the plasma membrane and nuclear lysosomal portions of the gradient during the first hour (Fig. 3A), similar to earlier findings in pancreatic acini and the pituitary gland (*24,25*). However, by 4 h (Fig. 3B) the greatest concentration remains in the low-density organelles, and by 24 h (Fig. 3C), somatostatin concentrations in the intracellular compartments overall are substantially decreased and show no preferential distribution in organelles. In contrast, the more degradation-resistant ^{125}I-WOC 4a and ^{111}In-pentetreotide show an early aggregation in low-density fractions at 1 h and appear concentrated predominantly in the nuclear lysosomal portion of the gradient by 24 h (Figs. 4 and 5).

To establish whether this progressive buildup in the higher density range of the gradient represents collection in lysosomes or nuclei, centrifugal precipitation of the nuclei

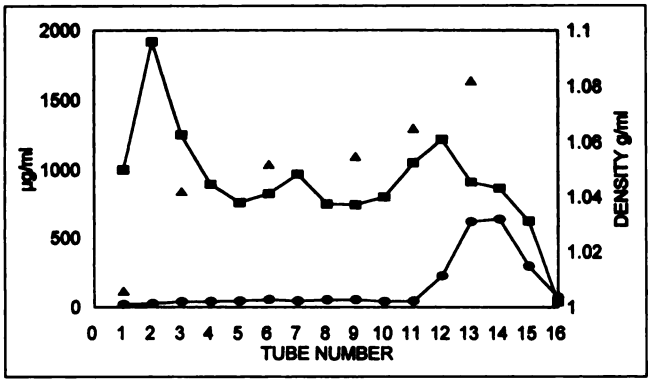

FIGURE 1. Plot of gradient density distributions of both DNA (●) and protein (■) from homogenized IMR-32 human neuroblastoma cells, with density distribution (▲) over gradient.

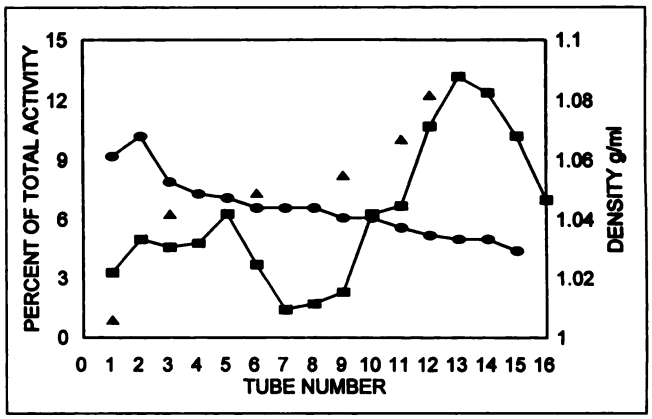

FIGURE 2. Plot of enzyme markers *N*-acetyl-β-glucosaminidase (■) and 5′ nucleotidase (●) after homogenization of IMR-32 neuroblastoma cells, with density distribution (▲) over gradient.

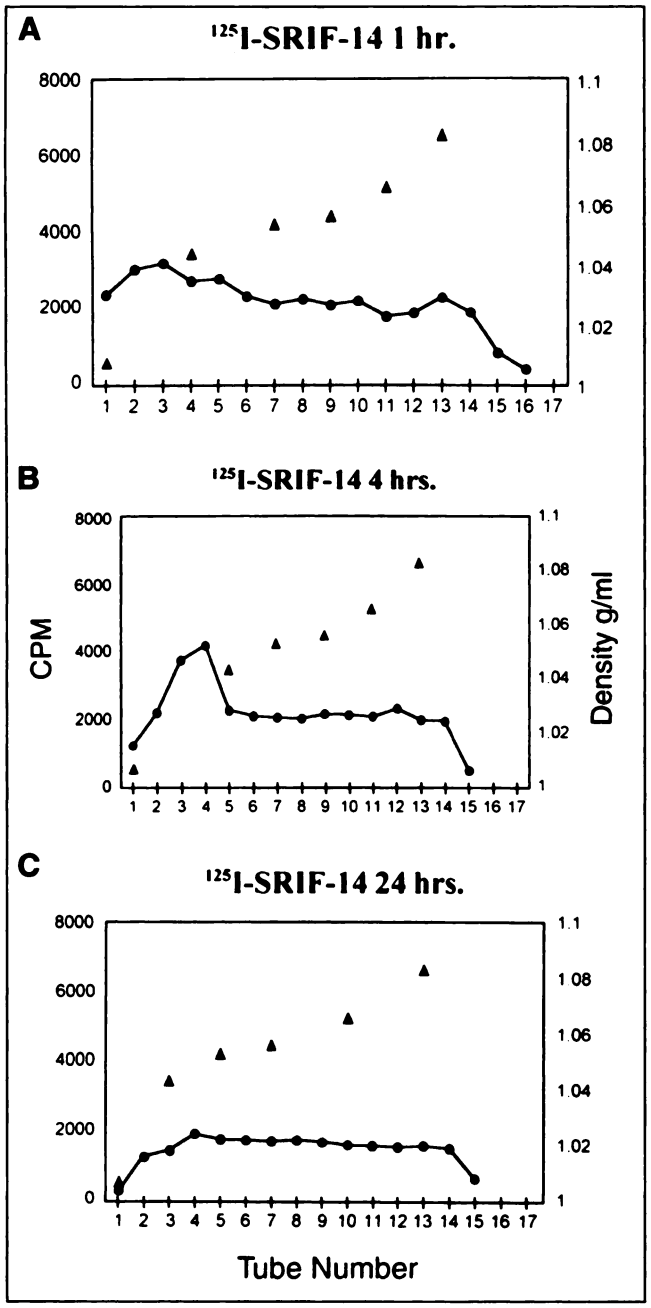

FIGURE 3. Plots of gradient density distributions over time of ^{125}I-somatostatin in human IMR-32 cell homogenates after incubation with ligand for either 1 (A), 4 (B), or 24 (C) h. Intracellular distribution of radioligand over time can be inferred by comparison with Figures 1 and 2.

was assessed spectrophotometrically (*20*). Each of the gradient figures has been selected as representative of between 3 and 6 individual experiments with the exception of experiments represented by Figure 6, which were performed in duplicate. Figure 6 plots a typical experiment, which included 24-h incubation with ^{125}I-WOC 4a; washing and homogenization of IMR-32 cells (*15*); division of homogenate into 2 equal portions, half of which was centrifuged at an average gravity of $400g_{av}$ for 10 min to precipitate nuclei; combination of both fractions with Percoll to form a 29% Percoll–sucrose mixture; and centrifugation, fractionation, and counting in a 5500 γ counter). The figure shows that approximately two thirds of the counts are lost with precipitation of the nuclei. This finding is confirmed by the counts recovered in the nuclear pellet (691,742 cpm), compared with the total gradient counts (1,071,786 cpm); the precipitation of more than 93% of the DNA; and the retention of more than 90% of the lysosomal enzyme

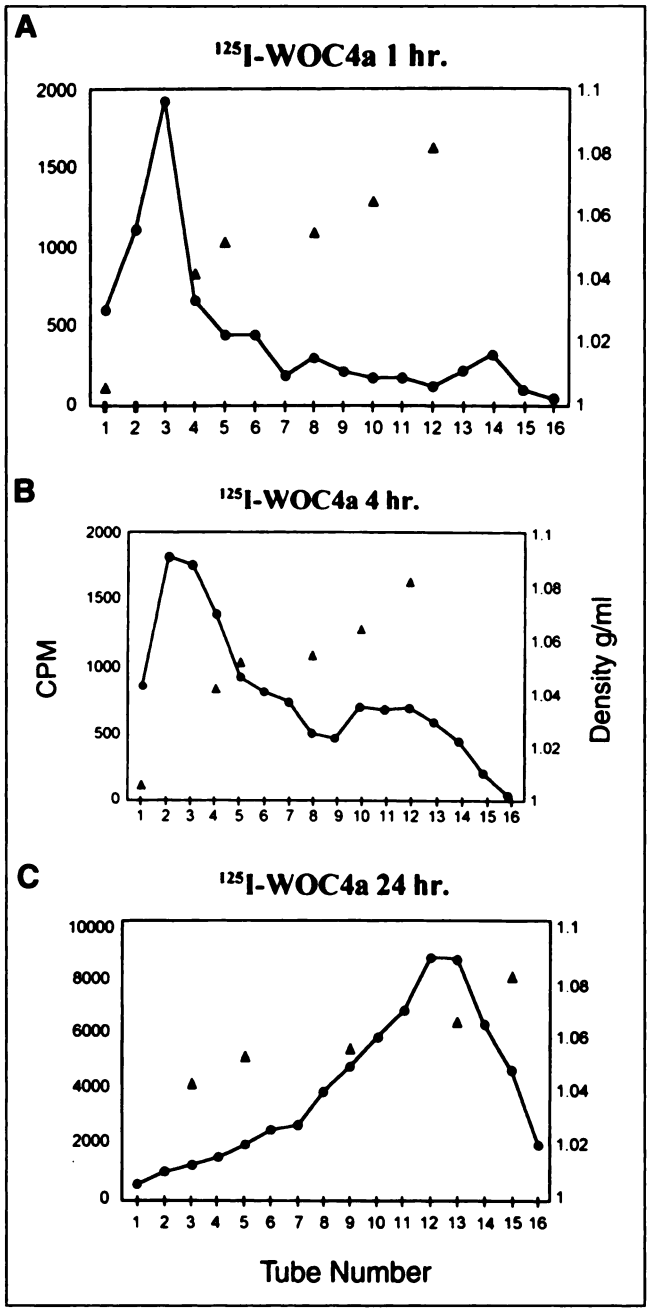

FIGURE 4. Plots of gradient density distributions over time of ^{125}I-WOC 4a in human IMR-32 cell homogenates after incubation with ligand for either 1 (A), 4 (B), or 24 (C) h. Intracellular distribution of radioligand over time can be inferred by comparison with Figures 1 and 2.

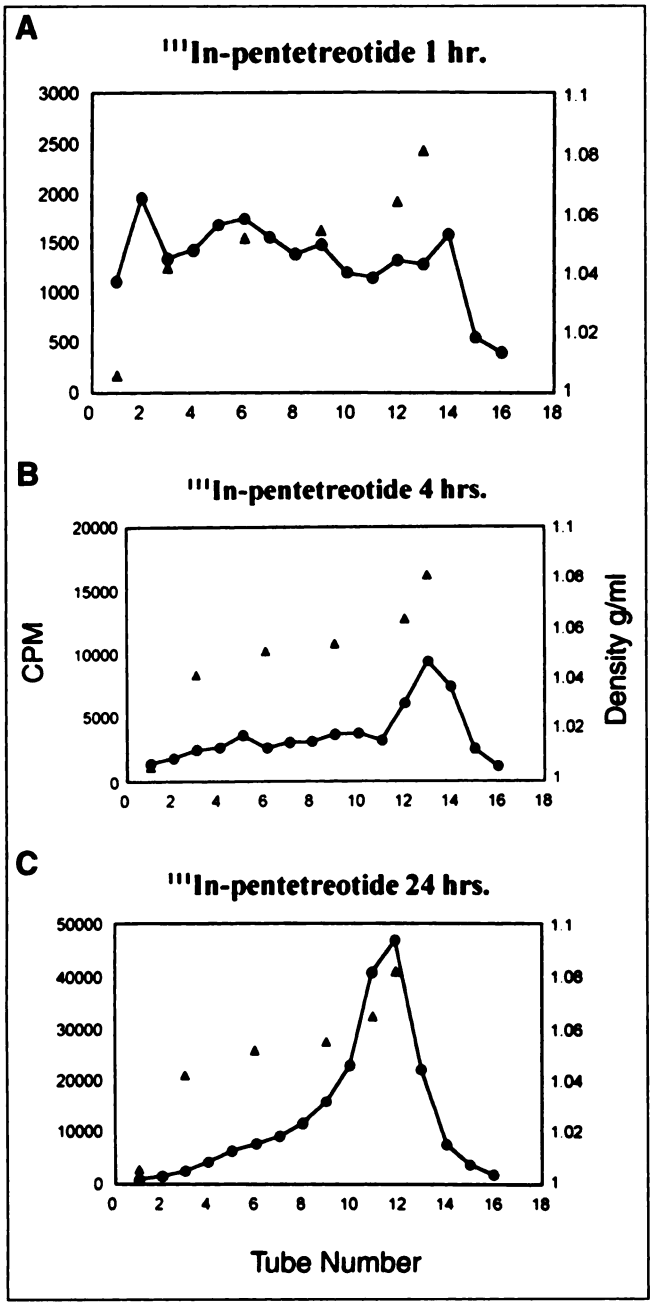

FIGURE 5. Plots of gradient density distributions over time of ^{111}In-pentetreotide in human IMR-32 cell homogenates after incubation with ligand for either 1 (A), 4 (B), or 24 (C) h. Intracellular distribution of radioligand over time can be inferred by comparison with Figures 1 and 2.

marker in the supernatant. A 24-h incubation of ^{111}In-pentetreotide and IMR-32 cells, both alone and with an excess of unlabeled competitor (octreotide), followed by homogenization and Percoll–sucrose gradient centrifugation (Fig. 7), shows that competition for binding and cellular uptake blocks the gradient distributions found in Figure 5. Moreover, when radiolabeled pentetreotide is added to the cellular homogenate immediately before gradient centrifugation, or to a Percoll–sucrose gradient with no cells present,

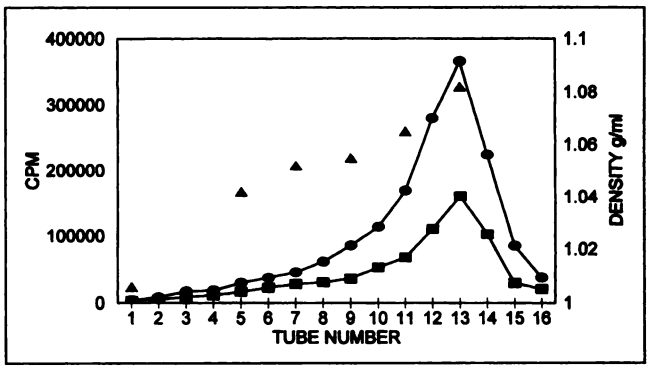

FIGURE 6. Plot of distribution of label on gradients with nuclei present (●) or absent (■). Density distribution in gradients was identical, as shown by marker beads (▲). Difference between plots represents nuclear localization of binding.

similar distributions of radiolabel are generated (Fig. 8). This finding indicates that the density distributions in Figures 3–5 require cellular uptake and intracellular transport and are not an artifact of centrifugation or the result of rebinding to the nuclear compartment of a label that had previously undergone endocytosis.

In this study, we show a progressive intracellular and nuclear accumulation of both iodine- and indium-labeled somatostatin analogs (Figs. 4 and 5). These observations show that the somatostatin analog rather than the radionuclide is the critical element required for internalization and nuclear transport of these radioligands. For evaluation of whether nuclear uptake was followed by interaction with DNA, DNA was obtained from IMR-32 (sst-2–positive) and SKNSH (sst-2–negative) cells after timed incubations with ^{111}In-pentetreotide. Figure 9 shows progressive DNA binding of ^{111}In-pentetreotide in IMR-32 cells incubated with radioligand alone and radioligand with an excess cold competitor, as well as a progressive rise in the specifically bound counts. In this analysis, triplicate flasks containing IMR-32 cells were incubated from 30 min to 48 h with

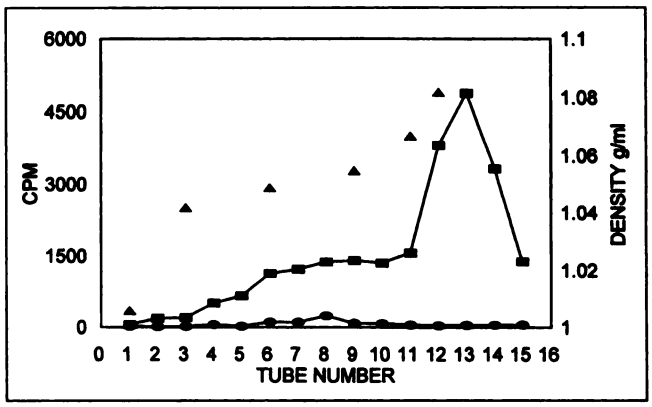

FIGURE 7. Plot of intracellular distributions of label for ^{111}In-pentetreotide alone (■) or with unlabeled competitor (●) after 24-h incubation of ^{111}In-pentetreotide in presence or absence of cold competitor (10^{-6} mol/L octreotide), followed by homogenization and fractionation of cells. Marker beads indicated gradient density distribution (▲).

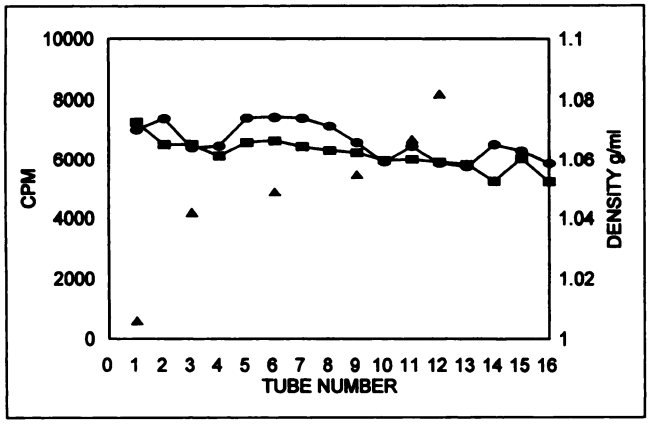

FIGURE 8. Plot of distribution of ^{111}In-pentetreotide in sequential fractions from Percoll (Sigma)–sucrose gradients determined in presence (●) or absence (■) of IMR-32 cellular homogenate.

^{111}In-pentetreotide in the presence or absence of 10^{-6} mol/L octreotide, harvested, and washed 3 times in Dulbecco's PBS. DNA was extracted from cells using a genomic preparation tissue DNA isolation kit. DNA from each flask was treated with proteinase for 1 h at 37°C and then precipitated again with 100% ethanol and 3 mol/L sodium acetate, washed in cold ethanol, and redissolved in 10 mmol/L Tris-EDTA, pH 7.4. The concentration of DNA in each sample was determined by spectrophotometry at 260 nm, 100 μg were transferred to counting vials, and the radioactivity associated with each tube was measured in a γ counter. Specific binding was calculated by subtracting label found in DNA in the presence of competitor from that found in DNA from cells incubated with label alone. Linear regression of specifically bound counts in DNA revealed an r of 0.967 and a P of 0.007, indicating a high degree of correlation between time of incubation and specific incorporation of radioligand into DNA fraction.

Similar analyses were performed on DNA isolated from somatostatin receptor–negative SKNSH cells. These cells failed to show significant uptake of ^{111}In-pentetreotide in their DNA fraction (Fig. 10). Both native somatostatin and its octreotide analog inhibit signal transduction and cell proliferation in IMR-32 cells after binding to a single class of high-affinity receptor sites (dissociation constants, 0.16 nmol/L and 0.89 nmol/L, respectively). In contrast, these compounds do not bind to SKNSH neuroblastoma cells, nor do they alter signal transduction or proliferation (*19*). The progressive rise in DNA-associated counts in somatostatin receptor–positive cells parallels the nuclear accumulation seen in Figure 3C.

DISCUSSION

Our data suggest that an additional destination for budding endosomal vesicles may be fusion with the nucleus. Alternatively, some form of transmembrane transport can enable somatostatin and its analogs to permeate the endosomal membrane, enter the cytoplasm, and either pass through both nuclear membranes or acquire transport through the nuclear pore complex. However, the mechanisms for transport out of endosomes and into the nucleus as well as possible intranuclear transduction events remain to be characterized.

Classically, somatostatin and its analogs were believed to bind to plasma membranes and to undergo limited internalization (2%–5%) during a short (1- to 4-h) incubation. Failure of Tyr^1-SRIF-14 to progressively accumulate in the nucleus may be caused by rapid deiodination by amino peptidases or cleavage of the Tyr^1 residue. Studies using ^{125}I-Tyr^{11}-SRIF are currently under way to determine if this form of native somatostatin will be internalized and transported to the nucleus. Our current data indicate that stable radiolabeled somatostatin analogs progressively accumulate in cells during prolonged exposures. In our studies, up to 80% of total cell-associated label is in the internalized fraction, and a large proportion of this radioactivity is translocated to the nucleus and subsequently to the DNA. Although a limited number of native cell lines have been

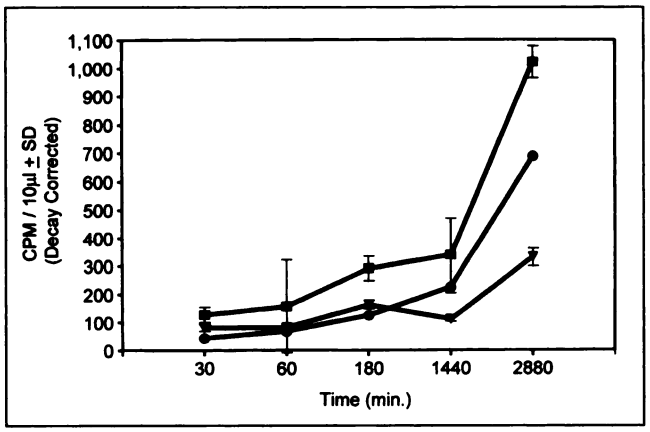

FIGURE 9. Plot of specific DNA binding (●) of ^{111}In-pentetreotide and binding in presence (▼) or absence (■) of cold competitor (10^{-6} mol/L octreotide).

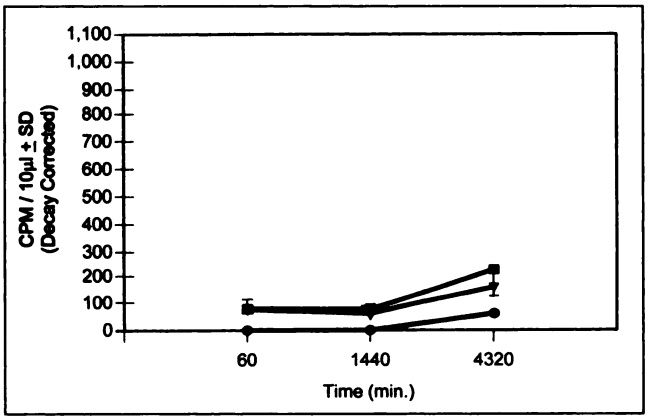

FIGURE 10. Plot of DNA from SKNSH shows little or no specific binding (●), determined as difference between label found in DNA in presence (▼) or absence (■) of cold competitor (10^{-6} mol/L octreotide). DNA was obtained from SKNSH human neuroblastoma cells using techniques outlined in Figure 7.

studied to date, the observations outlined here should be applicable to all cell lines with sst-2 and intact mechanisms for internalization. Earlier investigations showed that native somatostatin can also move to the nuclear compartment after binding and uptake (*24–26*). Accumulation of radiolabeled somatostatin analogs within the nuclei of cells and their increasing association with DNA over time may have significant clinical importance for in situ radiotherapy. Drug doses used in these in vitro studies are achievable in the clinical setting.

Radiolabeled peptides that specifically bind to DNA may allow for effective in situ radiation therapy with compounds that emit Auger electrons. In this study, we have shown the progressive intranuclear accumulation of Auger electron–emitting somatostatin analogs. In parallel studies, we have shown that these compounds effectively induce cytotoxicity in IMR-32 cells but not in PANC-1 (sst-2–negative) cells (*6*) or SKNSH cells. Progressive intracellular accumulation, nuclear translocation, and specific DNA binding of ^{111}In-pentetreotide or ^{125}I-WOC 4a in sst-2–expressing cells imply that internalization and subsequent translocation to the nucleus depend on the presence of membrane somatostatin receptors with intact endocytic mechanisms. The specific DNA sequence that binds pentetreotide and WOC 4a is unknown. The DNA extraction procedure used at least transiently denatures the DNA and disassociates naturally occurring DNA–protein complexes. We chose this relatively harsh extraction technique to learn of the association between the somatostatin analogs and DNA. We have not obtained solid evidence that the somatostatin analogs form covalent bonds with DNA, and it is not evident from the chemical nature of the radionuclides (^{125}I and ^{111}In) that either is chemically incorporated into the DNA structure. On the other hand, the radiolabeled somatostatin analogs, or some portion thereof, remain associated with nuclear DNA after extraction with chaotropic agents, implying a chemically strong bond. Experiments are in progress that will define the nature of the somatostatin–DNA association. A better understanding of this association may have considerable importance, allowing us to more accurately time clinical treatment and develop more effective DNA-targeted radiotherapeutic agents. Furthermore, we do not know if the somatostatin receptor is a part of the DNA binding complex. However, experiments that define the specific DNA binding sequence and determine if the somatostatin receptor is part of the DNA complex are currently under way in our laboratory.

Other experiments performed in our laboratory using freshly transfected SKR2 (an sst-2 transfected SKNSH cell line provided by M. Sue O'Dorisio) have shown higher membrane binding than with IMR-32 cells but significant impairment of internalization compared with IMR-32. This result suggests that these cells may have a defect in the endocytic machinery (e.g., an inability to cluster in coated pits) necessary for effective internalization and intranuclear accumulation.

Nuclear concentration and DNA binding of stable somatostatin analogs should enable radioligands that emit Auger electrons, such as ^{111}In and ^{125}I, to be used for in situ radiotherapy in tumors possessing both high densities of somatostatin receptors and intact signal transduction pathways. Clinical results from pilot trials of these concepts are encouraging (*8,23*).

Furthermore, a pilot trial comparing tumor and whole-body accumulation and retention of radiolabeled somatostatin analogs administered by bolus and by prolonged (24- to 72-h) infusions seems to support our observations (*27*).

ACKNOWLEDGMENTS

The authors thank George J. Drouant and Joseph A. Fuselier for radiolabeling and purifying the peptides used in this study.

REFERENCES

1. Reisine T, Bell GI. Molecular biology of somatostatin receptors. *Endocr Rev.* 1995;16:427–442.
2. Patel YC, Greenwood MT, Warszynska A, Panetta R, Srikant CB. All five cloned human somatostatin receptors are functionally coupled to adenyl cyclase. *Biochem Biophys Res Commun.* 1994;198:605–612.
3. Lamberts SW, Krenning EP, Klijn JG, Reubi JC. The clinical use of somatostatin analogs in the treatment of cancer. *Baillieres Clin Endocrinol Metab.* 1990;4: 29–49.
4. Reubi JC, Laissue J, Krenning EP, Lamberts SW. Somatostatin receptors in human cancer: incidence, characteristics, functional correlates and clinical implications. *J Steroid Biochem Mol Biol.* 1992;43:27–35.
5. Woltering EA, O'Dorisio MS, O'Dorisio TM. The role of radiolabeled somatostatin analogs in the management of cancer patients. In: DeVita VT Jr, Hellman S, Rosenberg SA, eds. *Principles and Practice of Oncology.* Philadelphia, PA: Lippincott-Raven; 1995:1–16.
6. McCarthy KE, Woltering EA, Espenan GD, Cronin M. In situ radiotherapy with ^{111}In-pentetreotide: initial observations and future directions. *Cancer J Sci Am.* 1998;4:94–102.
7. Meyers MO, Anthony CT, O'Dorisio TM, et al. Multiply radioiodinated somatostatin analogs induce receptor specific cytotoxicity. *J Surg Res.* 1998;76:154–158.
8. Krenning EP, Kooij PP, Bakker WH, et al. Radiotherapy with a radiolabeled somatostatin analog, (^{111}In-STPA-D-Phe^1)-octreotide: a case history. *Ann NY Acad Sci.* 1994;733:496–506.
9. Sahu SK, Baranowska-Kortylewicz J, Taube RA, Adelstein SJ, Kassis AL. Strand breaks after the decay of iodine-125 in proximity to plasmid pBR322 DNA. *Radiat Res.* 1997;147:401–408.
10. Humm JL, Howell RW, Rao DV. Dosimetry of Auger-electron emitting radionuclides: report no. 3 of AAPM Nuclear Medicine Task Group No. 6. *Med Phys.* 1994;21:1901–1915.
11. Amherdt M, Patel YC, Orci L. Binding and internalization of somatostatin, insulin, and glucagon by cultured rat islet cells. *J Clin Invest.* 1989;84:412–417.
12. Hornick CA, Hui DY, DeLamatre JG. A role for retrosomes in intracellular cholesterol transport from endosomes to the plasma membrane. *Am J Physiol.* 1997;273:C1075–C1081.
13. Brown WJ, Farquhar MG. The mannose phosphate receptor for lysosomal enzymes is concentrated in cis golgi cisternae. *Cell.* 1984;36:295–307.
14. Apodaca G, Katz LA, Mostov KE. Receptor mediated transcytosis of IgA in MDCK cells is via apical recycling endosomes. *J Cell Biol.* 1994;125:67–86.
15. Roth A, Kreienkamp HJ, Nehring RB, Roosterman D, Meyerhof W, Richter D. Endocytosis of the rat somatostatin receptors: subtype discrimination, ligand specificity, and delineation of carboxy-terminal positive and negative sequence motifs. *DNA Cell Biol.* 1997;16:111–119.
16. Nouel D, Gaudriault G, Houle M, et al. Differential internalization of somatostatin in COS-7 cells transfected with SST-1 and SST-2 receptor subtypes: a confocal microscopic study using novel fluorescent somatostatin derivatives. *Endocrinology.* 1997;138:296–306.
17. Koenig, JA, Edwardson JM, Humphrey PP. Somatostatin receptors in Neuro2A neuroblastoma cells: ligand internalization. *Br J Pharmacol.* 1997;120:52–59.
18. Hukovic N, Panetta R, Kumar U, Patel YC. Agonist-dependent regulation of cloned human somatostatin receptor type sw 1-5 (hSSTR1-5): subtype selective internalization or upregulation. *Endocrinology.* 1996;137:4046–4049.

19. O'Dorisio MS, Chen F, O'Dorisio TM, Wrang D, Qualman SJ. Characterization of somatostatin receptors on human neuroblastoma tumors. *Cell Growth Differ.* 1991;5:1–8.
20. Khoury G, Lai CJ. Preparation of simian virus 40 and its DNA. In: Jakoby WB, Pastan IM, eds. *Methods in Enzymology.* Vol 57. New York, NY: Academic Press; 1978:404–412.
21. Emmelot PC, Bos J, Benedetti EL, Rumke PH. Studies on plasma membranes: 1. Chemical composition and enzyme content of plasma membranes isolated from rat liver. *Biochem Biophys Acta.* 1964;90:126–145.
22. Findlay JG, Levy A, Marsh CA. Inhibition of glycosidases by aldonolactones of corresponding configuration. *Biochem J.* 1958;69:467–476.
23. Woltering EA, O'Dorisio MS, Murphy WA, et al. Synthesis and characterization of multiply-tyrosinated, multiply-iodinated somatostatin analogs. *J Peptide Res.* 1999;53:201–213.
24. Viguerie N, Esteve JP, Susiini C, Vaysse N, Ribet A. Processing of receptor-bound somatostatin: internalization and degradation by pancreatic acini. *Am J Physiol.* 1987;252:G535–G542.
25. Morel G, Pelletier G, Heisler S. Internalization and distribution of radiolabeled somatostatin-28 in mouse anterior pituitary tumor cells. *Endocrinology.* 1986;119: 1972–1979.
26. Morel G. Internalization and nuclear localization of peptide hormones. *Biochemical Pharm.* 1994;47:63–76.
27. Espenan GD, Nelson JA, Fisher DR, et al. Experiences with high-dose radiopeptide therapy: the health physics perspective. *Health Phys.* 1999;76:225–235.